



Reconstruction of the atmospheric $^{39}\text{Ar}/\text{Ar}$ history

Ji-Qiang Gu^a, Amin L. Tong^a, Guo-Min Yang^a, Shui-Ming Hu^a, Wei Jiang^{a,*}, Zheng-Tian Lu^a, Roland Purtschert^b, Florian Ritterbusch^a

^a Hefei National Laboratory for Physical Sciences at the Microscale, CAS Center for Excellence in Quantum Information and Quantum Physics, University of Science and Technology of China, 96 Jinzhai Road, Hefei 230026, China

^b Climate and Environmental Physics Division, Physics Institute, University of Bern, Bern CH-3012, Switzerland

ARTICLE INFO

Editor: Christian France-Lanord

Keywords:

^{39}Ar dating
 Anthropogenic ^{39}Ar production
 Cosmogenic ^{39}Ar production
 ^{39}Ar input function
 Atom Trap Trace Analysis

ABSTRACT

The radioactive isotope ^{39}Ar is an ideal tracer for ocean ventilation, groundwater flow, and for dating mountain glaciers. With a half-life of 269 years, it covers the age range from a few tens to about 1800 years. We evaluate the input history of the atmospheric ^{39}Ar in the past 2500 years. By measuring the $^{39}\text{Ar}/\text{Ar}$ ratios of a modern argon sample and two old argon samples collected in 1959 and 1961, respectively, the anthropogenic contribution to the atmospheric ^{39}Ar in the past 60 years is determined to be less than 15%. The temporal variation of the atmospheric ^{39}Ar in the past 2500 years is calculated based on a cosmic-ray record derived from ice cores and tree rings. It is found that the atmospheric $^{39}\text{Ar}/\text{Ar}$ ratio has changed by as much as 17% in that period of time. This input variation has to be taken into account and corrected for in future ^{39}Ar dating applications.

1. Introduction

^{39}Ar is a cosmogenic radioactive isotope that can be used as an environmental tracer. As a noble gas isotope ^{39}Ar is chemically inert and homogeneously distributed in the atmosphere. With a half-life of 269 years, ^{39}Ar covers an existing dating gap between the applicable range of ^{14}C dating and that of young-age tracers including ^3H and ^{85}Kr (Loosli, 1983). Moreover, it is suitable for studying mixing processes in the ocean. ^{39}Ar combined with ^{14}C can provide constraints on the Transit Time Distribution (TTD), an effective method for the characterization of the degree of mixing (Hall and Plumb, 1994; Waugh et al., 2003). Therefore, it is a powerful tool in ocean current and ocean ventilation studies (Schlosser et al., 1994; Broecker and Peng, 2000; Holzer and Primeau, 2010). Besides applications in ocean studies, ^{39}Ar also has important applications in dating mountain glaciers and groundwater. In the past ^{39}Ar was mainly measured with the Low-Level Decay Counting (LLC) method in groundwater studies, where typically 1–2 tons of water were degassed in the field (Avrahamov et al., 2018; Yechieli et al., 2019; Markovich et al., 2021). The advent of the Atom Trap Trace Analysis (ATTA) technique has enabled ^{39}Ar analysis with only a few kilograms of ocean water or ice (Ebser et al., 2018; Feng et al., 2019). Presently, only two laboratories can perform such measurements, one at Heidelberg University (Ritterbusch et al., 2014) and the other is our laboratory at the University of Science and Technology of China. The precision of the

analysis is about 5% at the moment for 1–2 mL STP of argon sample.

For cosmogenic ^{39}Ar dating, it is important to know the $^{39}\text{Ar}/\text{Ar}$ input history in the atmosphere and the possible anthropogenic contributions. The atmospheric ^{39}Ar is mainly produced by cosmic rays in the stratosphere via the $^{40}\text{Ar}(n,2n)^{39}\text{Ar}$ reaction. The contributions of $^{38}\text{Ar}(n,\gamma)^{39}\text{Ar}$, $^{40}\text{Ar}(\gamma,n)^{39}\text{Ar}$ and $^{40}\text{Ar}(\mu^-,n)^{39}\text{Ar}$ reactions in the atmosphere are negligible (Loosli and Oeschger, 1968). A uniform global atmospheric ^{39}Ar concentrations is expected because its half-life as well as residence time in air are long compared to time scales involved in atmospheric mixing processes (Lal and Peters, 1967; Loosli, 1983). However, the production rate of ^{39}Ar in the atmosphere varies with time along with the cosmic-ray flux. It was estimated that the $^{39}\text{Ar}/\text{Ar}$ ratio in the atmosphere may have changed by up to 7% in the last 1000 years (Oeschger et al., 1974; Loosli, 1983). In deep underground and in high-uranium and -thorium rocks, ^{39}Ar is mainly produced through the $^{39}\text{K}(n,p)^{39}\text{Ar}$ reaction (Loosli et al., 1989; Sramek et al., 2017). In shallow depths cosmic-ray muon capture through the $^{39}\text{K}(\mu^-, \nu_\mu)^{39}\text{Ar}$ reaction may also play a role (Mei et al., 2010). Nucleogenic ^{39}Ar production can affect radiometric groundwater ages if the release rate of ^{39}Ar from rocks to the water is significant. Therefore, one should take these effects into account when using ^{39}Ar dating in the study of hydrological processes of groundwater systems (Yokochi et al., 2013). However, the release of ^{39}Ar from the subsurface to the atmosphere is negligible compared to the cosmogenic production. So ice core or ocean

* Corresponding author.

E-mail address: wjiang1@ustc.edu.cn (W. Jiang).

<https://doi.org/10.1016/j.chemgeo.2021.120480>

Received 29 April 2021; Received in revised form 2 August 2021; Accepted 12 August 2021

Available online 14 August 2021

0009-2541/© 2021 Published by Elsevier B.V.

water dating are not affected by the subsurface production. Besides the naturally produced ^{39}Ar , anthropogenic ^{39}Ar has been produced and released into the atmosphere since the dawn of the nuclear age. Potential anthropogenic sources of ^{39}Ar include testing of nuclear devices and other human nuclear activities. The 14.1 MeV neutrons produced in the deuterium-tritium reaction have enough energy to produce ^{39}Ar by the $^{40}\text{Ar}(n, 2n)^{39}\text{Ar}$ reaction (Loosli and Oeschger, 1968; Nolte et al., 2006). Loosli (1983) measured argon samples collected during 1940–1979 and set an upper limit of 5% - 7% modern for a possible anthropogenic contribution to the tropospheric ^{39}Ar activity.

Previous evaluations on the $^{39}\text{Ar}/\text{Ar}$ input history in the atmosphere and its effect on ^{39}Ar -dating have been done with the LLC method (Loosli and Oeschger, 1968; Loosli, 1983). However, the high analytical precision of the ATTA technique has decreased the sample size and increased measurement precision, thus raising demands for a reevaluation of the input history of $^{39}\text{Ar}/\text{Ar}$ in the atmosphere. The purpose of this paper is, therefore, to provide a quantitative estimation of naturally and anthropogenically induced variations of the atmospheric $^{39}\text{Ar}/\text{Ar}$ ratio.

The paper is organized as follows. In Section 2, we discuss the relation between the cosmic-ray flux and the production of ^{39}Ar in the atmosphere followed by an estimation of the input history of atmospheric $^{39}\text{Ar}/\text{Ar}$ based on a reconstructed cosmic ray record. In Section 3 we present a comparison of measurements of $^{39}\text{Ar}/\text{Ar}$ ratios in a modern argon sample and two old argon samples collected from the air in 1959 and 1961, respectively. This measurement sets constraints on anthropogenic ^{39}Ar released in the last 60 years. The measurements in this study were performed with the ATTA method which is briefly introduced in Sections 3.1 and 3.2. In Section 3.3, the experimental results are compared to theoretical estimations. Finally the implications on ^{39}Ar dating and an outlook for future improvement and directions are given.

2. Cosmic-ray flux history and the input function of ^{39}Ar

The input function of atmospheric ^{39}Ar can be inferred from the cosmic ray flux history. As the primary cosmic rays, which consist mostly of protons, cascade down the atmosphere, showers of secondary particles will be produced with a large fraction of neutrons, which interact with the atmosphere and produce e.g. ^{39}Ar , ^{14}C , ^{10}Be , etc. The general form of the production rate of a cosmogenic isotope at altitude D in the atmosphere is given by (Masarik and Beer, 1999),

$$P(D, M, \Phi) = \sum_i N_i \sum_k \int_0^\infty \sigma_{ik}(E_k) \cdot J_k(E_k, D, M, \Phi) dE_k \quad (1)$$

where N_i is the number of atoms for target element i per kg material in the atmosphere, $\sigma_{ik}(E_k)$ is the cross section for the production of the isotope from the target element i by particles of type k with energy E_k , and $J_k(E_k, D, M, \Phi)$ is the total flux of particles of type k with energy E_k at altitude D for the geomagnetic field M and the solar modulation parameter Φ .

The general behavior of the production cross section for most of the cosmogenic isotopes are quite similar. The isotopes are mainly produced by the reaction between neutrons and the stable isotopes in the atmosphere (N, O and Ar) (Lal and Peters, 1967). Therefore, there is a strong correlation between the neutron flux in the atmosphere and the abundance of the cosmogenic radionuclides. This relation is particularly useful in the study of cosmic radiation history and the input function of cosmogenic radioisotopes. On one hand, a well preserved cosmogenic radionuclide records, e.g. ^{14}C from tree rings or ^{10}Be from ice cores, can be used as neutron monitor and a proxy for cosmic-ray intensity (Steinhilber et al., 2012; Beer et al., 2013). On the other hand, the inferred cosmic-ray record can be used to estimate the historical variation of a cosmogenic radioisotope in the atmosphere.

In the following, we will calculate the atmospheric $^{39}\text{Ar}/\text{Ar}$ input function based on a reconstructed cosmic ray intensity record. From

analyses of stable and radioactive isotopes in meteorites of different size, it is concluded that the energy spectra of galactic cosmic radiation during the past hundreds of millions of years remained constant (Honda and Arnold, 1964). The production rate of ^{39}Ar in the air is therefore directly related to the incoming cosmic-ray particle flux which varies in space and time due to variations of (i) the solar irradiance (McCracken et al., 2002; Beer et al., 2013) and (ii) the shielding effect of the Earth's magnetic field (Carcaillet et al., 2003; Beer et al., 2013). In order to calculate the temporal evolution of atmospheric ^{39}Ar , its reservoir and sinks also need to be considered. Owing to the chemical inertness and being a gas, the main ^{39}Ar reservoir is the atmosphere. The upper layer of the ocean equilibrates with the atmosphere in one month (Broecker and Peng, 2000). Due to the low solubility of argon in water and the relatively slow diffusive and advective mixing of surface water with the deep ocean, less than 1% of the global Ar inventory is dissolved in the ocean, which has negligible effect on the atmospheric ^{39}Ar (Lal and Peters, 1967). The only major sink of ^{39}Ar in the atmosphere is through radioactive decay. Therefore, the number of ^{39}Ar atoms in the atmosphere N_{39} at time t_0 is the decay weighted average of the cosmogenic ^{39}Ar production from the past to t_0 ,

$$N_{39}(t_0) = \int_{t_0}^\infty P(t) \cdot e^{-\frac{(t-t_0)}{\tau}} dt \quad (2)$$

where $P(t)$ is the production rate [atom/a] and τ the mean life-time of ^{39}Ar [a]. Due to exponential decay, the integration can be cut off at a finite time T when $T-t_0 \gg \tau$. The contributions before T become negligible. The atmospheric $^{39}\text{Ar}/\text{Ar}$ input function we wish to calculate is the variation of $^{39}\text{Ar}/\text{Ar}$ relative to its value in the modern atmosphere, i.e. it is a normalized $^{39}\text{Ar}/\text{Ar}$ ratio,

$$\begin{aligned} (^{39}\text{Ar}/\text{Ar})_{\text{norm}}(t_0) &= \frac{N_{39}(t_0)/N_{40}(t_0)}{N_{39}(0)/N_{40}(0)} \\ &= \int_{t_0}^\infty P(t) \cdot e^{-\frac{(t-t_0)}{\tau}} dt \Big/ \int_0^\infty P(t) \cdot e^{-\frac{(t-t_0)}{\tau}} dt \end{aligned} \quad (3)$$

Here $N_{40}(0) = N_{40}(t_0)$ is used, i.e. the number of ^{40}Ar atoms in the atmosphere over the past few thousand years can be considered constant (Bender et al., 2008). For the ^{39}Ar production rate, the normalized cosmic-ray intensity record reconstructed from Steinhilber et al. (2012) is used. This record extends back to 9400 years BP (before present where present refers to 1950 CE). It is long enough for the estimation of ^{39}Ar input function in the last 2500 years, a time span that is relevant for ^{39}Ar dating applications. This normalized cosmic-ray record is obtained from the ^{10}Be ice core records from Greenland and Antarctica as well as the global ^{14}C tree ring records. By combining these records and performing the principal component analysis (PCA), the cosmic-ray intensity (22-year averages) based on the first principal component is extracted for the past 9400 years. The average uncertainty of the PCA analysis is about 5%. Since the cosmic-ray record is much longer than the half-life of ^{39}Ar , the variations before 9400 years BP have no effect on the input function between 0 and 2500 years, the duration relevant to ^{39}Ar dating.

The reconstructed isotopic $^{39}\text{Ar}/\text{Ar}$ abundance normalized by the modern value is plotted in Fig. 1, along with the normalized cosmic-ray intensity in the past 2500 years. Here, the normalized $^{39}\text{Ar}/\text{Ar}$ ratio is plotted because, for ^{39}Ar dating and many other dating applications, it is adequate to have the knowledge about the abundance relative to a standard sample (in our case the modern Ar). The long-term variation of the cosmic ray intensity is due to the changing geomagnetic dipole shielding of the Earth. The cosmic radiation fluctuations on centennial time scales are mostly due to solar modulation (Steinhilber et al., 2012). Compared with the cosmic-ray intensity, the ^{39}Ar concentration in the atmosphere is much smoother, because ^{39}Ar can stay in the atmosphere for hundreds of years thus the centennial variation of its concentration is largely averaged out. However, the slow change due to the variation of the geomagnetic dipole field strength still persists. The calculation

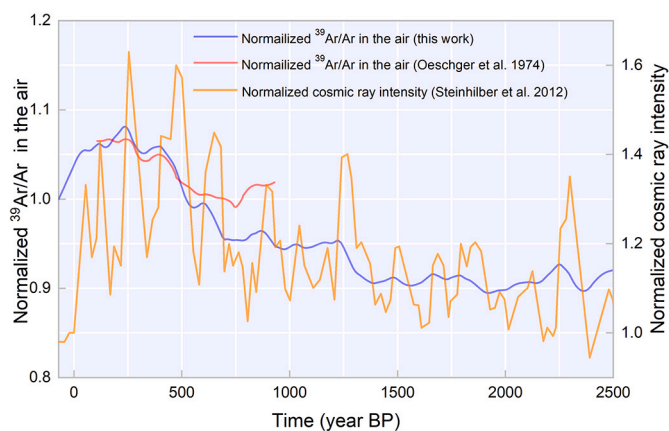


Fig. 1. The $^{39}\text{Ar}/\text{Ar}$ ratio in the air normalized to its value in the modern air (blue curve) and normalized cosmic-ray intensity (orange curve) in the past 2500 years. Time is given as year before present (BP where present refers to 1950 CE). The cosmic ray intensity data is from Steinhilber et al. (2012). It is normalized to the value at 0 year BP. The red curve is a previous estimation based on ^{14}C data in tree rings by Oeschger et al. (1974). The difference between the blue and red curves are mainly due to the different cosmic ray records used in the calculations. (For interpretation of the references to colour in this figure legend, the reader is referred to the web version of this article.)

shows that the variation of the atmospheric $^{39}\text{Ar}/\text{Ar}$ ratio is about 17% in the past 2500 years.

3. Constraints on the anthropogenic ^{39}Ar contribution in the modern atmosphere

In order to evaluate the contribution of anthropogenic ^{39}Ar in the modern atmosphere, we acquired two argon samples extracted from the air in 1959 and 1961, respectively. N_2 and O_2 are not found in these Ar samples indicating no air leak during the long storage time. We use the historical record of nuclear tests to give an estimation of the anthropogenic ^{39}Ar in these samples. Fig. 2 shows the yield of the atmospheric nuclear detonation from 1950 to 2010 (Hua and Barbetti, 2004). This record can be used as an estimation of neutrons produced in these tests.

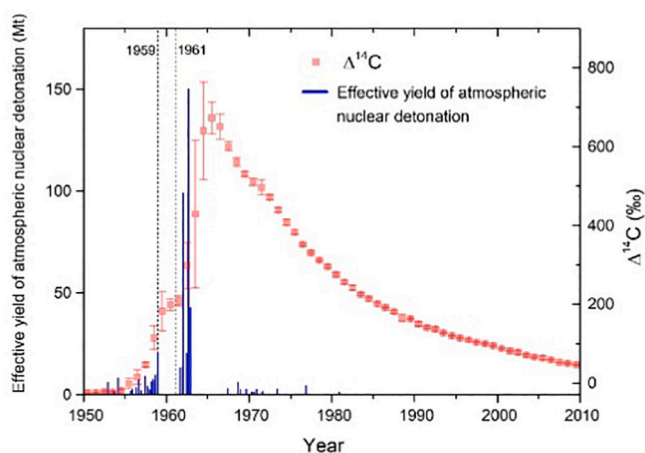


Fig. 2. Atmospheric ^{14}C record and the magnitude of atmospheric nuclear detonation from 1950 to 2010. The red points are atmospheric ^{14}C records. Blue bars represent effective yield of atmospheric nuclear detonations in three-month periods (for 1950–1976, Enting, 1982; for 1977–1980, Yang et al., 2000). Data taken from Hua and Barbetti (2004) and Hua et al. (2013). The dashed lines mark the collection times of the two argon samples used in this study. (For interpretation of the references to colour in this figure legend, the reader is referred to the web version of this article.)

Since the $(n, 2n)$ reaction on ^{40}Ar is the dominant pathway for anthropogenic ^{39}Ar production, the amount of ^{39}Ar produced is, in first order approximation, proportional to the yield of these tests. Because the “bomb peaks” appear in 1962 and 1963, these two argon samples collected before that time should have relatively small anthropogenic contributions. This can also be seen in the atmospheric bomb ^{14}C record, which should have a similar shape to the anthropogenic ^{39}Ar production curve because the neutrons spectrum needed for ^{14}C and ^{39}Ar production are similar (Hua and Barbetti, 2004; Hua et al., 2013). The record shows that the atmospheric ^{14}C started to increase in the mid-1950s. At 1959 and 1961 the anthropogenic contribution became visible but it is still 4 to 5 times smaller than the later bomb peak around 1963. After 1965 the atmospheric ^{14}C slowly drops towards its pre-bomb value due to rapid exchange between the atmosphere, oceans, and biosphere (Hua and Barbetti, 2004).

Based on the above estimations the 1959 and 1961 argon samples are used as our reference with minor anthropogenic contributions. The $^{39}\text{Ar}/\text{Ar}$ ratio of these samples are measured and compared with a modern argon sample we purchased in 2018 (This sample is referred to as the “modern sample” throughout the paper). The newly developed ATTA apparatus for ^{39}Ar at the University of Science and Technology is used for these measurements. The objective of this study is to extend constraints on the anthropogenic production of ^{39}Ar in the last 60 years, a time span that is both different and longer than the previous works (Loosli and Oeschger, 1968; Loosli, 1983).

3.1. The Atom Trap Trace Analysis method

Atom Trap Trace Analysis (ATTA) method has been successfully used to measure ^{85}Kr and ^{81}Kr (Chen et al., 1999; Jiang et al., 2012; Lu et al., 2014). The analysis on ^{39}Ar based on the same principle is more challenging because the isotopic abundance of ^{39}Ar is 8×10^{-16} , much lower than that of either ^{81}Kr or ^{85}Kr , which will result in an atom count rate 1000 times lower. Nevertheless, demonstration work on ^{39}Ar detection with ATTA was performed and later developments have achieved atom counting rate up to 7 atoms/h. These developments eventually enabled analysis of ^{39}Ar on small environmental samples (Jiang et al., 2011; Ritterbusch et al., 2014; Ebser et al., 2018; Feng et al., 2019).

At the University of Science and Technology of China, an ATTA apparatus dedicated for ^{39}Ar dating was built recently. The principles of ATTA can be found in several publications (Jiang et al., 2011; Jiang et al., 2012; Lu et al., 2014; Ritterbusch et al., 2014). The system is capable of capturing and counting individual ^{39}Ar atoms in an argon sample down to 10^{-17} level and determining its isotopic abundance. Through optimizing system parameters, an atom counting rate of 10 atoms/h for modern argon samples is achieved. The new ATTA apparatus also features measurements on ^{38}Ar as the reference isotope. The $^{39}\text{Ar}/^{38}\text{Ar}$ ratio is measured during the analysis (Due to different measurement techniques used for ^{39}Ar and ^{38}Ar , arb. Units is used. (Tong et al., 2021)). This ratio is insensitive to any common changes of the system, such as slow drifts of the capture efficiency of the atom trap system.

3.2. Samples and measurement procedure

The measurements of the samples are conducted in the following manner. 1–2 mL STP of argon gas are released into the vacuum system and are recirculated. Each measurement takes about 20 h. During the measurement, the laser frequencies automatically switch between ^{39}Ar and ^{38}Ar in 10.5-min cycles (10 min on ^{39}Ar and 0.5 min on ^{38}Ar). The switching time between two isotopes is faster than the time scale of slow efficiency drifts of the system. By taking the ratio between the signals of ^{39}Ar and ^{38}Ar , the effects of the varying counting efficiency, common to both isotopes, can largely be cancelled (Tong et al., 2021).

The three argon samples are measured in the course of 40 days, with each sample measured seven times. A rotating measurement scheme is

adopted. This scheme evenly distributes the measurements for each sample during the whole experiment in order to average out the effect of any potential slow systematic drift of the ATTA system. Upon completion of each measurement, the sample inside the system is pumped away. Before introducing new samples for the next measurement, the system is cleaned with a xenon discharge for more than 10 h. By this process the implanted ^{39}Ar from the previous sample is released from the walls, which reduces the cross-sample contamination down to less than 1%.

3.3. Results and constraints on the anthropogenic ^{39}Ar input

Fig. 3a shows the $^{39}\text{Ar}/^{38}\text{Ar}$ ratios of the three argon samples measured over time. Most of the measurements have uncertainties of about 7% (20-h measurement for each point), which are dominated by the counting statistics of ^{39}Ar . The ATTA system shows reproducibility and stability over the entire data taking period thanks to the ^{38}Ar referencing technique. The measurements for each sample are all consistent within the measurement uncertainties (reduced Chi-squared are all close to 1). The $^{39}\text{Ar}/^{38}\text{Ar}$ ratios of the 1959 and 1961 samples are noticeably lower than the modern argon sample because of the radioactive decay of ^{39}Ar . As 60 years have passed since the collection of these samples, the ^{39}Ar concentration in these old samples has dropped to about 85% of their original values. To make comparison among these samples, we make the weighted average of the seven measurements for each sample and adjust the $^{39}\text{Ar}/^{38}\text{Ar}$ ratio to that of its collection date. The result is shown in Fig. 3b. The relative uncertainty for each point is about 3%. To get a quantitative estimation of the anthropogenic contribution to the atmospheric ^{39}Ar since 1961, we take the weighted average of the $^{39}\text{Ar}/^{38}\text{Ar}$ ratios of the 1959 and 1961 samples and use it as the reference with little anthropogenic contributions (2.92 ± 0.07 , see Table 1). With this $^{39}\text{Ar}/^{38}\text{Ar}$ ratio of the old argon samples and the ^{39}Ar input function shown in Fig. 1 we can infer the $^{39}\text{Ar}/^{38}\text{Ar}$ ratio in the

Table 1
Weighted average of the $^{39}\text{Ar}/^{38}\text{Ar}$ ratios for the three Ar samples.

Sample #	$^{39}\text{Ar}/^{38}\text{Ar}$ (a.u.) (weighted average)	$^{39}\text{Ar}/^{38}\text{Ar}$ ratio (a.u.) (weighted average, decay corrected)
Ar modern	3.00 ± 0.09	3.02 ± 0.09
Ar 1959	2.44 ± 0.08	2.86 ± 0.09
Ar 1961	2.58 ± 0.08	3.00 ± 0.09
Ar 1959, 1961 combined	–	2.92 ± 0.07

modern atmosphere with sole cosmogenic origin. The atmospheric $^{39}\text{Ar}/^{38}\text{Ar}$ ratio with cosmogenic origin in year 2018 (time when our commercial modern argon was produced) is about 3.2% smaller than the value in 1959–1961 (See Fig. 1). Its value is calculated to be 2.83 ± 0.16 and is denoted as $(^{39}\text{Ar}/^{38}\text{Ar})_{\text{cosmo_modern}}$. The enlarged standard error includes the uncertainty of the input history curve in Fig. 1. The $^{39}\text{Ar}/^{38}\text{Ar}$ of the modern argon sample measured in our experiment has both cosmogenic and anthropogenic contributions. This ratio is denoted as $(^{39}\text{Ar}/^{38}\text{Ar})_{\text{total_modern}}$.

To constrain the anthropogenic contribution to the atmospheric ^{39}Ar in the last 60 years their super ratio (i.e. the ratio of ratios) is calculated. The result is

$$\frac{(^{39}\text{Ar}/^{38}\text{Ar})_{\text{total_modern}}}{(^{39}\text{Ar}/^{38}\text{Ar})_{\text{cosmo_modern}}} = 1.07 \pm 0.07.$$

From this result, the anthropogenic contribution is estimated to be less than 15% of the cosmogenic ^{39}Ar in the modern atmosphere with 90% confidence (using a standard deviation of 0.07). This means the number of ^{39}Ar atoms produced in the nuclear tests is less than 1.4×10^{26} . This value can be compared to the calculation based on the neutron yield of all nuclear tests which is about 8×10^{28} (total yield of the nuclear tests ~ 400 Mt., the average neutron yield is 2×10^{26} neutron/Mt) (Yang et al., 2000; Naegler and Levin, 2006). As an upper limit estimate we simply assume that the energy of all neutrons is 14.1 MeV (neutron energy from the D-T reaction), which is high enough for the $^{40}\text{Ar}(n, 2n)^{39}\text{Ar}$ reaction. Among these neutrons, about 2×10^{-3} can produce ^{39}Ar atoms in the atmosphere (Loosli and Oeschger, 1968). This rough estimation results in a maximal number of anthropogenic ^{39}Ar in the atmosphere of 2×10^{26} , which is in line with the experimental limit given above.

4. Conclusion

The input history of ^{39}Ar in the atmosphere presented in this work can be used in ^{39}Ar dating applications. We calculated the input function corrected ^{39}Ar ages and compare the results with the ^{39}Ar ages obtained with no input function correction (assuming constant ^{39}Ar abundance in the air). The results are shown in Fig. 4. The age correction ranges from -43 to $+30$ years in the past 2500 years. The uncertainties of the age correction curve and the $^{39}\text{Ar}/\text{Ar}$ input history are inherited from the cosmic-ray record used in the calculation.

As the development for ^{39}Ar analytical method continues, more works related to this study are expected in the future. Based on the estimations in this work the anthropogenic contributions to the atmospheric $^{39}\text{Ar}/\text{Ar}$ could be at the level of a few percent, which could be detected by future measurements with greater analytical precisions. Measurements on well-dated ice cores with known gas-ice age differences may further reduce the uncertainties of the input history of ^{39}Ar in the atmosphere. It may also provide additional constraints to the variation of the cosmic-ray fluxes in the past millennium complementing the ^{14}C and the ^{10}Be isotopes.

Declaration of Competing Interest

The authors declare that they have no known competing financial

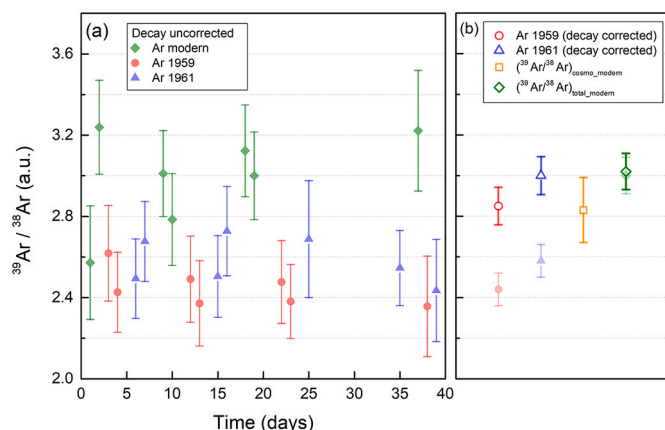


Fig. 3. (a) The $^{39}\text{Ar}/^{38}\text{Ar}$ ratios of the modern Ar sample and the two Ar samples collected from the air in 1959 and 1961, respectively, measured with the ATTA method. Due to the radioactive decay of ^{39}Ar , the $^{39}\text{Ar}/^{38}\text{Ar}$ ratios of the two old Ar samples are noticeably lower than the modern Ar sample. (b) The weighted averages of the $^{39}\text{Ar}/^{38}\text{Ar}$ ratios of the three samples (decay uncorrected, solid symbols). The ratios are adjusted to the values at the collection times (decay corrected, open symbols). The decay corrected $^{39}\text{Ar}/^{38}\text{Ar}$ ratios of the 1959 and 1961 samples are averaged and adjusted according to the ^{39}Ar input function (Fig. 1) to give an estimation of the $^{39}\text{Ar}/^{38}\text{Ar}$ in the modern atmosphere with cosmogenic origin (open orange square). The decay corrected $^{39}\text{Ar}/^{38}\text{Ar}$ ratio of the modern Ar sample (open green diamond) has both cosmogenic and anthropogenic contributions. By comparing these two ratios the anthropogenic contributions to the atmospheric ^{39}Ar is limited to be less than 15% (see text and Table 1 for details). (For interpretation of the references to colour in this figure legend, the reader is referred to the web version of this article.)

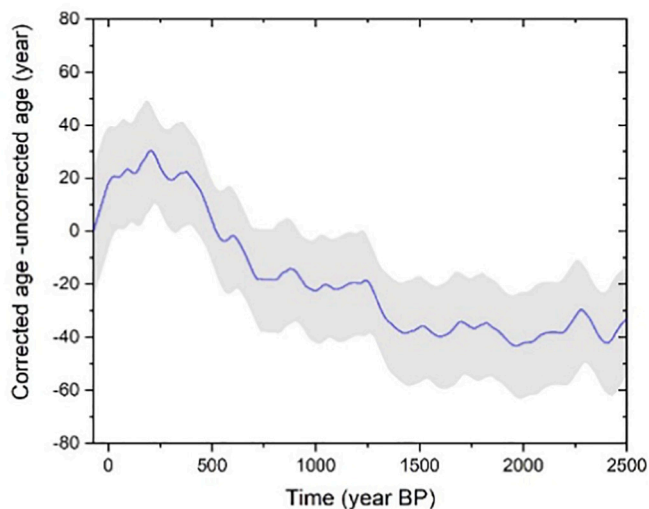


Fig. 4. Age correction curve for ^{39}Ar dating due to input variations of the atmospheric $^{39}\text{Ar}/\text{Ar}$ ratio. A typical 5% uncertainty on the input function of ^{39}Ar is used to calculate the uncertainty band of the age correction curve.

interests or personal relationships that could have appeared to influence the work reported in this paper.

Acknowledgments

This work is funded by the National Key Research and Development Program of China (Grant No. 2016YFA0302200); National Natural Science Foundation of China (Grants No. 41727901, No. 41861224007, and No. 41961144027); and Anhui Initiative in Quantum Information Technologies (Grant No. AHY110000). Data available at doi:<https://doi.org/10.5281/zenodo.4727509>

References

- Avrahamov, N., Yechieli, Y., Purtschert, R., Levy, Y., Sültenfuß, J., Vergnaud, V., Burg, A., 2018. Characterization of a carbonate karstic aquifer flow system using multiple radioactive noble gases (^3H - ^3He , ^{85}Kr , ^{39}Ar) and ^{14}C as environmental tracers. *Geochim. Cosmochim. Acta* 242, 213–232. <https://doi.org/10.1016/j.gca.2018.09.009>.
- Beer, J., McCracken, K.G., Abreu, J., Heikkilä, U., Steinhilber, F., 2013. Cosmogenic radionuclides as an extension of the neutron monitor era into the past: potential and limitations. *Space Sci. Rev.* 176, 89–100. <https://doi.org/10.1007/s11214-011-9843-3>.
- Bender, M., Barnett, B., Dreyfus, G., Jouzel, J., Porcelli, D., 2008. The contemporary degassing rate of ^{40}Ar from the solid Earth. *PNAS* 105 (24), 8232–8237. <https://doi.org/10.1073/pnas.0711679105>.
- Broecker, W.S., Peng, T.-H., 2000. Comparison of ^{39}Ar and ^{14}C ages for waters in the deep ocean. *Nucl. Instr. Meth. Phys. Res. B* 172, 473–478. [https://doi.org/10.1016/S0168-583X\(00\)00272-X](https://doi.org/10.1016/S0168-583X(00)00272-X).
- Carcaillet, J.T., Thouveny, N., Bourles, D.L., 2003. Geomagnetic moment instability between 0.6 and 1.3 Ma from cosmogenic evidence. *Geophys. Res. Lett.* 30, 1792. <https://doi.org/10.1029/2003GL017550>.
- Chen, C.Y., Li, Y.M., Bailey, K., O'Connor, T.P., Young, L., Lu, Z.-T., 1999. Ultrasensitive isotope trace analysis with a magneto-optical trap. *Science* 286, 1139–1141. <https://doi.org/10.1126/science.286.5442.1139>.
- Ebser, S., Kersting, A., Stöven, T., Feng, Z., Ringena, L., Schmidt, M., Tanhua, T., Aeschbach, W., Oberthaler, M.K., 2018. ^{39}Ar dating with small samples provides new key constraints on ocean ventilation. *Nat. Commun.* 9, 5046. <https://doi.org/10.1038/s41467-018-07465-7>.
- Enting, I.G., 1982. Nuclear weapons data for use in carbon cycle modeling. In: CSIRO Division of Atmospheric Physics Technical Paper No. 44. Melbourne: CSIRO.
- Feng, Z., Bohlender, P., Ebser, S., Ringena, L., Schmidt, M., Kersting, A., Hopkins, P., Hoffmann, H., Fischer, A., Aeschbach, W., Oberthaler, M.K., 2019. Dating glacier ice of the last millennium by quantum technology. *Proc. Natl. Acad. Sci. U. S. A.* 116, 8781–8786. <https://doi.org/10.1073/pnas.1816468116>.
- Hall, T.M., Plumb, R.A., 1994. Age as a diagnostic of stratospheric transport. *J. Geophys. Res.-Atmos.* 99, 1059–1070. <https://doi.org/10.1029/93JD03192>.
- Holzer, M., Primeau, F., 2010. Improved constraints on transit time distributions from argon 39: a maximum entropy approach. *J. Geophys. Res.* 115, C12021. <https://doi.org/10.1029/2010JC006410>.

- Honda, M., Arnold, A.R., 1964. Effects of Cosmic Rays on Meteorites Science, 143, p. 203. <https://doi.org/10.1126/science.143.3603.203>.
- Hua, Q., Barbetti, M., 2004. Review of tropospheric bomb radiocarbon data for carbon cycle modeling and age calibration purposes. *Radiocarbon* 46, 1273–1298. <https://doi.org/10.1017/S0033822200033142>.
- Hua, Q., Barbetti, M., Rakowski, A.Z., 2013. Atmospheric radiocarbon for the period 1950–2010. *Radiocarbon* 55, 2059–2072. https://doi.org/10.2458/azu_js_rc.v55i2.16177.
- Jiang, W., Williams, W., Bailey, K., Davis, A.M., Hu, S.-M., Lu, Z.-T., O'Connor, T.P., Purtschert, R., Sturchio, N.C., Sun, Y.R., Mueller, P., 2011. ^{39}Ar detection at the 10^{-16} isotopic abundance level with atom trap trace analysis. *Phys. Rev. Lett.* 10, 103001. <https://doi.org/10.1103/PhysRevLett.106.103001>.
- Jiang, W., Bailey, K., Lu, Z.-T., Mueller, P., O'Connor, T.P., Cheng, C.-F., Hu, S.-M., Purtschert, R., Sturchio, N.C., Sun, Y.R., Williams, W.D., Yang, G.-M., 2012. An atom counter for measuring ^{81}Kr and ^{85}Kr in environmental samples. *Geochim. Cosmochim. Acta* 91, 1–6. <https://doi.org/10.1016/j.gca.2012.05.019>.
- Lal, D., Peters, B., 1967. Cosmic ray produced radioactivity on the earth. In: Sitte, K. (Ed.), *Kosmische Strahlung II/Cosmic Rays II. Handbuch der Physik/Encyclopedia of Physics*, vol 9/46/2. Springer, Berlin, Heidelberg. https://doi.org/10.1007/978-3-642-46079-1_7.
- Loosli, H.H., 1983. A dating method with ^{39}Ar . *Earth Planet. Sci. Lett.* 63 (1), 51–62. [https://doi.org/10.1016/0012-821X\(83\)90021-3](https://doi.org/10.1016/0012-821X(83)90021-3).
- Loosli, H.H., Oeschger, H., 1968. Detection of ^{39}Ar in atmospheric Ar. *Earth Planet. Sci. Lett.* 5, 191–198. [https://doi.org/10.1016/S0012-821X\(68\)80039-1](https://doi.org/10.1016/S0012-821X(68)80039-1).
- Loosli, H.H., Lehmann, B.E., Balderer, W., 1989. Argon-39, argon-37 and krypton-85 isotopes in Stripa groundwaters. *Geochim. Cosmochim. Acta* 53, 1825–1829. [https://doi.org/10.1016/0016-7037\(89\)90303-7](https://doi.org/10.1016/0016-7037(89)90303-7).
- Lu, Z.-T., Schlosser, P., Smethie Jr., W.M., Sturchio, N.C., Fischer, T.P., Kennedy, B.M., Purtschert, R., Severinghaus, J.P., Solomon, D.K., Tanhua, T., Yokochi, R., 2014. Tracer applications of noble gas radionuclides in the geosciences. *Earth-Sci. Rev.* 138, 196–214. <https://doi.org/10.1016/j.earscirev.2013.09.002>.
- Markovich, K.H., Condon, L.E., Carroll, K.C., Purtschert, R., McIntosh, J.C., 2021. A mountain-front recharge component characterization approach combining groundwater age distributions, noble gas thermometry, and fluid and energy transport modeling. *Water Resour. Res.* 57. <https://doi.org/10.1029/2020WR027743>.
- Masarik, J., Beer, J., 1999. Simulation of particle fluxes and cosmogenic nuclide production in the Earth's atmosphere. *J. Geophys. Res.* 104 (D10), 12099–12111. <https://doi.org/10.1029/1998jd200091>.
- McCracken, K.G., Beer, J., McDonald, F.B., 2002. A five-year variability in the modulation of the galactic cosmic radiation over epochs of low solar activity. *Geophys. Res. Lett.* 29, 2161. <https://doi.org/10.1029/2002GL015786>.
- Mei, D.-M., Yin, Z.-B., Spaans, J., Koppang, M., Hime, A., Keller, C., Gehman, V.M., 2010. Prediction of underground argon content for dark matter experiments. *Phys. Rev. C* 81, 055802. <https://doi.org/10.1103/PhysRevC.81.055802>.
- Naegler, T., Levin, I., 2006. Closing the global radiocarbon budget 1945–2005. *J. Geophys. Res.* 111, D12311. <https://doi.org/10.1029/2005JD006758>.
- Nolte, E., Rühm, W., Loosli, H.H., Tolstikhin, I., Kato, K., Huber, R.C., Egbert, S.D., 2006. Measurements of fast neutrons in Hiroshima by use of ^{39}Ar . *Tecton. Environ. Biophys.* 44, 261–271. <https://doi.org/10.1007/s00411-005-0025-0>.
- Oeschger, H., Gugelmann, A., Loosli, H.H., Schotterer, U., Siegenthaler, U., Wiest, W., 1974. ^{39}Ar dating of groundwater in isotope techniques. In: *Groundwater Hydrology*, vol. II. IAEA, Vienna, pp. 179–190, 11–15 March 1974.
- Ritterbusch, F., Ebser, S., Welte, J., Reichel, T., Kersting, A., Purtschert, R., Aeschbach, W., Oberthaler, M.K., 2014. Groundwater dating with Atom Trap Trace Analysis of ^{39}Ar . *Geophys. Res. Lett.* 41, 6758–6764. <https://doi.org/10.1002/2014GL061120>.
- Schlosser, P., Kromer, B., Weppernig, R., Loosli, H.H., Bayer, R., Bonani, G., Suter, M., 1994. The distribution of ^{14}C and ^{39}Ar in the Weddell. *J. Geophys. Res.-Oceans* 99, 10275–10287. <https://doi.org/10.1029/94JC00313>.
- Sramek, O., Stevens, L., McDonough, W.F., Mukhopadhyay, S., Peterson, R.J., 2017. Subterranean production of neutrons, ^{39}Ar and ^{21}Ne : rates and uncertainties. *Geochim. Cosmochim. Acta* 196, 370–387. <https://doi.org/10.1016/j.gca.2016.09.040>.
- Steinhilber, F., Abreu, J.A., Beer, J., Brunner, I., Christl, M., Fischer, H., Heikkilä, U., Kubik, P.W., Mann, M., McCracken, K.G., Miller, H., Miyahara, H., Oerter, H., Wilhelm, F., 2012. 9,400 years of cosmic radiation and solar activity from ice cores and tree rings. *Proc. Natl. Acad. Sci. U. S. A.* 109, 5967–5971. <https://doi.org/10.1073/pnas.1118965109>.
- Tong, A.L., Gu, J.-Q., Yang, G.-M., Hu, S.-M., Jiang, W., Lu, Z.-T., Ritterbusch, F., 2021. An atom trap system for ^{39}Ar dating with improved precision. *Rev. Sci. Instrum.* 92, 063204. <https://doi.org/10.1063/5.0050620>.
- Waugh, D.W., Hall, T.M., Haine, T.W.N., 2003. Relationships among tracer ages. *J. Geophys. Res.-Oceans* 108, 3138. <https://doi.org/10.1029/2002JC001325>.
- Yang, X., North, R., Rommey, C., 2000. CMR Nuclear Explosion Database (Revision 3). CMR Technical Report CMR-00/16.
- Yechieli, Y., Yokochi, R., Zilberbrand, M., Lu, Z.-T., Purtschert, R., Sueltenfuss, J., Jiang, W., Zappala, J., Mueller, P., Bernier, R., Avrahamov, N., Adar, E., Talhami, F., Livshitz, Y., Burg, A., 2019. Recent seawater intrusion into deep aquifer determined by the radioactive noble-gas isotopes ^{81}Kr and ^{39}Ar . *Earth Planet. Sci. Lett.* 507, 21–29. <https://doi.org/10.1016/j.epsl.2018.11.028>.
- Yokochi, R., Sturchio, N.C., Purtschert, R., Jiang, W., Lu, Z.-T., Mueller, P., Yang, G.-M., Kennedy, B.M., Kharaka, Y., 2013. Noble gas radionuclides in Yellowstone geothermal gas emissions: a reconnaissance. *Chem. Geol.* 339, 43–51. <https://doi.org/10.1016/j.chemgeo.2012.09.037>.